

TADEUSZ BIELA

Polish Academy of Sciences, Center of Molecular and Macromolecular Studies  
Department of Polymer Chemistry  
ul. Sienkiewicza 112, 90-363 Łódź, Poland  
e-mail: tadek@bilbo.cbmm.lodz.pl

## Stereocomplexes of star-shaped poly[(*R*)-lactide]s and poly[(*S*)-lactide]s bearing various number of arms. Synthesis and thermal properties

**Summary** — Stereocomplexes composed of 6, ~13, 24 and 32 arm star-shaped poly(lactide)s (ss-sc-PLAs) and of the mixed star-shaped — linear PLAs (sl-sc-PLAs) were prepared in a controlled way. Their thermal properties were characterized by DSC and compared to their linear counterparts properties. It was observed that the equimolar mixtures of star-shaped (*R*)-PLA and (*S*)-PLA crystallize during precipitation into methanol from the methylene chloride solution preferentially in the form of the highly crystalline (up to 70 %) stereocomplexes. The star-shaped PLA stereocomplexes with the number of arms higher than six (*i.e.* ~13, 24 and 32) survived melting and after slow cooling during the second heating run crystallized once again showing exclusive stereocomplex formation. After melting and annealing at high temperature and then fast cooling to the room temperature, in the second heating run also only two peaks in thermograms appeared exothermic cold crystallization peak ( $T_{ccsc}$ ) and endothermic melting peak ( $T_{msc}$ ) for star-shaped sc-PLAs with ~13, 24 and 32 arms. For high molar mass linear, mixed star-shaped — linear and six arm star-shaped stereocomplexes additional (*R*)-PLA and (*S*)-PLA homo-crystallites melting peaks appeared. These results show that thermal stability of stereocomplexes is strongly influenced by the topology and the number of arms in the star-shaped components.

**Key words:** star-shaped polylactides, stereocomplexes, differential scanning calorimetry, thermal properties.

### STEREOKOMPLEKSY POLI (*R*)- I POLI (*S*)-LAKTYDÓW GWIAŹDZISTYCH ZAWIERAJĄCYCH RÓŻNĄ LICZBĘ RAMION. SYNTEZA I WŁAŚCIWOŚCI TERMICZNE

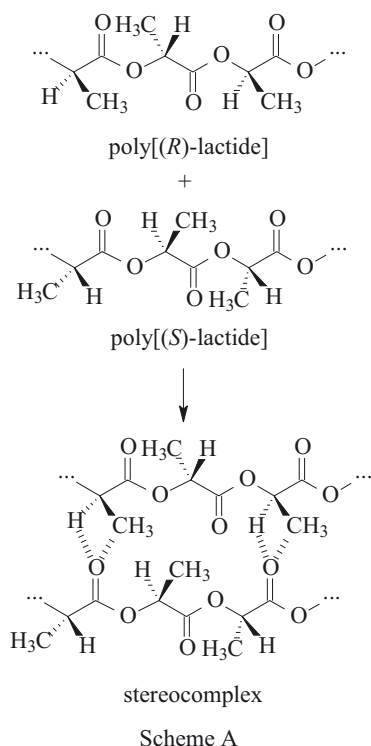
**Streszczenie** — Zsyntetyzowano stereokompleksy polilaktydów o strukturze gwiazdzystej zawierających 6, ~13, 24 i 32 ramiona (ss-sc-PLAs) oraz stereokompleksy mieszane polilaktydów gwiazdzystych i liniowych. Charakterystykę wyjściowych polilaktydów zawiera tabela 1. Właściwości termiczne otrzymanych mieszanin określono metodą skaningowej kalorymetrii różnicowej (DSC) i porównano je z właściwościami odpowiednich stereokompleksów liniowych (tabele 2 i 3, rys. 2—9 i 11). Zaobserwowano, że wytrącenie równomolowej mieszaniny gwiazdzystych polilaktydów (*R*)-PLA i (*S*)-PLA w dichlorometanie do metanolu prowadzi do wysoce krystalicznego stereokompleksu (stopień krystaliczności >70 %). Stereokompleksy polilaktydów gwiazdzystych o liczbie ramion przekraczającej sześć (*tj.* ~13, 24 i 32) są zdolne do przetrwania stopienia i po powolnym ochłodzeniu, podczas drugiego cyklu ogrzewania w toku analizy DSC krystalizują wyłącznie w postaci stereokompleksu. Również wówczas, gdy stereokompleksy gwiazdzystych polilaktydów zawierających ~13, 24 i 32 ramiona stopi się i wygrzeje w wysokiej temperaturze, a następnie szybko schłodzi do temperatury pokojowej, to podczas drugiego ogrzewania w termogramach występują wyłącznie dwa piki — egzotermiczny zimnej krystalizacji ( $T_{ccsc}$ ) i endotermiczny topnienia ( $T_{msc}$ ). Natomiast w termogramach stereokompleksów polilaktydów liniowych, liniowo-gwiazdzystych i gwiazdzystych lecz zawierających tylko sześć ramion pojawiają się dodatkowe piki związane z topnieniem homokrystalitów (*R*)-PLA i (*S*)-PLA. Otrzymane wyniki wskazują na silną zależność odporności cieplnej stereokompleksów polilaktydowych od topologii tworzących je komponentów (rys. 10 i 12).

**Słowa kluczowe:** polilaktydy gwiazdziste, stereokompleksy, skaningowa kalorymetria różnicowa, właściwości cieplne.

Poly(lactide)s (PLAs) — (bio)degradable and biocompatible polymers prepared from renewable resources, have recently become the industrial reality

[1—5]. PLA have an asymmetric carbon atom in each lactate repeating unit and depending on the monomer used in polymerization — (*R,R*)-lactide, (*S,S*)-lactide,

racemic [1:1 (*R,R*)/(*S,S*)-lactide] or meso (*R,S*)-lactide — semicrystalline (*S*)-PLA and (*R*)-PLA or amorphous (*S,R*)-PLA polymers are obtained. The intermolecular interactions of enantiomeric PLA chains of the opposite configuration [(*R*)-PLA and (*S*)-PLA] lead to the corresponding stereocomplexes (sc-PLAs) formation. This stereogenic interaction between (*R*)-PLA and (*S*)-PLA has been reported for the first time by Tsuji and Ikada [6]. Initially, van der Waals bonds were proposed to be responsible for stereocomplex formation, but more recently a weak hydrogen bonding:  $-\text{CH}_3\cdots\text{O}=\text{C}-$  and  $\equiv\text{CH}\cdots\text{O}=\text{C}-$  between the (*R*)-PLA/(*S*)-PLA chains has been found to keep two PLA helical chains with the opposite configuration together [7, 8].



Thermal properties of stereocomplex crystallites are different from those of crystallites composed of either (*R*)-PLA or (*S*)-PLA enantiomer (homochiral crystallites). Thus,  $T_m$  of the high molar mass linear (*R*)-PLA or (*S*)-PLA does not exceed 180 °C whereas of  $T_m$  of sc-PLA is reaching 230 °C [6, 9–13].

However, all of the stereocomplex investigations were limited till now to the linear polylactides. For stereocomplexes based on star-shaped or hyper-branched polymers an enhancement of some physical properties could be expected because of multiarm topology of the interacting components.

Preparation of high melting, stable polymeric stereocomplexes based on the high molar mass polylactides seems to be important from the technological viewpoint. Stereocomplexes of the linear, high molar mass (*R*)-PLA and (*S*)-PLA are known to be not able to reform quantitatively back from the melt in any reasonable time. The ability of restoring stereocomplexes during thermal

treatment decreases with increasing their molar mass. It has particularly been observed that for macromolecules with molar mass ( $M_n$ ) above  $\sim 10^4$  g/mol crystallites of homochiral (*R*)-PLA, (*S*)-PLA components coexist with crystallites of the (*R*)-PLA/(*S*)-PLA stereocomplex when pure stereocomplexes are melted and then crystallized once again. Only for macromolecules with  $M_n \leq 10^4$  g/mol the homochiral crystallites may be absent. These are the  $M_n$  below threshold needed for practical applications of PLA as thermoplastic material. The actual proportions of both crystalline structures depend on the methods of preparation, the experimental conditions of the melting/cooling runs, and on further annealing.

The present paper follows short communication published by us recently [14].

## EXPERIMENTAL

### Materials

Tin(II) octoate (2-ethylhexanoate) [ $\text{Sn}(\text{Oct})_2$  commercial product from Sigma, Aldrich] was purified by two consecutive high vacuum distillations at 140 °C/ $3 \cdot 10^{-3}$  mbar. Thus purified  $\text{Sn}(\text{Oct})_2$ , stored on the vacuum line, was finally distributed directly into the thin-walled vials or ampoules equipped with breakseals, then sealed off and stored at -12 °C.

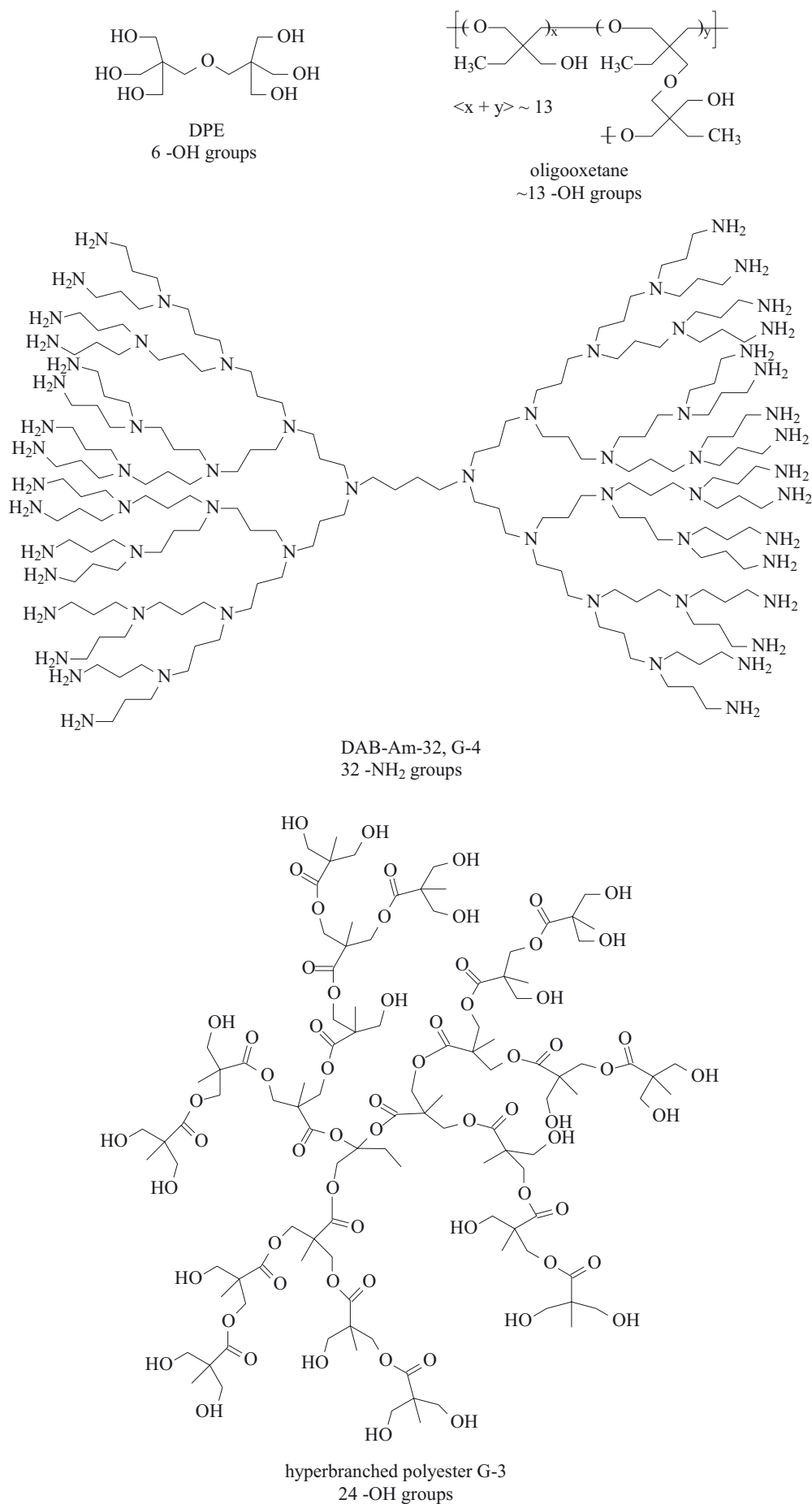
(*S,S*)-Lactide (LA, from Boehringer Ingelheim, Germany) and (*R,R*)-lactide (99 %, Purac, Netherlands) crystallized consecutively from dry 2-propanol and toluene, were purified just before use by sublimation in *vacuo* ( $10^{-3}$  mbar, 85 °C).

The monofunctional initiator BuOH (from Aldrich, 99 %) was distilled under atmosphere pressure from Na chips and then distributed under vacuum into thin-walled vials.

The following multifunctional initiators containing either -OH or -NH<sub>2</sub> groups were used: dipentaerithritol (DPE) with 6-OH groups (from Perstorp AB, Sweden); DAB-Am-32, polypropylenimine dotriacontamine, generation 4.0 with 32-NH<sub>2</sub> groups (from Aldrich); oligooxetane with  $\sim 13$ -OH groups; and hyperbranched aliphatic polyesters based on 2,2-bis(hydroxymethyl)propionic acid and trimethylolpropane (TMP) dendrimer, generation 3.0 terminated with 24-OH. Structures of the cores used as initiators are presented in the Scheme B. Initiators were melted and dried under vacuum before use. Syntheses of oligooxetane and hyperbranched polyesters were already described [15, 16].

Tetrahydrofuran (THF, POCH, Gliwice, Poland, 99 %) was kept for several days over KOH pellets, filtered off and refluxed over Na metal. Eventually it was distilled, degassed and stored over liquid Na/K alloy, developed blue color.

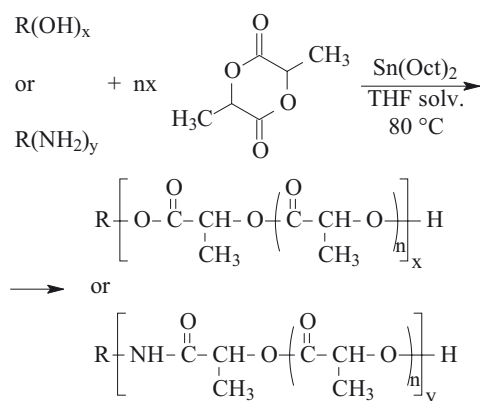
Methylene chloride ( $\text{CH}_2\text{Cl}_2$ , POCH, Gliwice, Poland, 99 %) was dried with calcium chloride and distilled before use.



Methanol (POCH, Gliwice, Poland, pure p. a. grade) was used as received.

### Polymerization

The linear and star-shaped (*R*)-PLA and (*S*)-PLA — enantiomeric (homochiral) polymers have been synthesized according to the known procedure [17–21] employing the ring-opening polymerization of (*R,R*)- and (*S,S*)-lactides respectively (Scheme C).



where  $x$  is equal to 1, 6, ~13 or 24 and  $y$  is equal to 32

Scheme C

Namely, (*R,R*)-lactide and (*S,S*)-lactide monomers were polymerized in bulk at 120 °C or in THF solution at 80 °C with Sn(Oct)<sub>2</sub> and monofunctional (BuOH) in the case of linear PLAs or appropriate multifunctional initiator (with 6, ~13, 24, and 32 -OH or -NH<sub>2</sub> groups) in the case of star-shaped PLAs as components of the catalytic/initiating system. Polymerizing mixtures were prepared in sealed glass ampoules using standard high vacuum technique. Progress of polymerization was followed by means of <sup>1</sup>H NMR and SEC.

A general procedure follows example described below. Sn(Oct)<sub>2</sub> (1 mL of 0.25 mol · L<sup>-1</sup> solution in dry THF) and (*S,S*)-LA (14.87 g, 103 mmol) were transferred under vacuum into breakseals and sealed after freezing in liquid N<sub>2</sub>. Dipentaerythritol (DPE) (0.0378 g, 1.49 · 10<sup>-1</sup> mmol) was put into thin-walled vial, melted and dried under vacuum, then sealed after freezing in liquid N<sub>2</sub>. Breakseals containing Sn(Oct)<sub>2</sub>/THF solution and (*S,S*)-LA monomer and tube with immersed DPE vial were sealed to the reaction (~10 mL) glass vessel. Breakseals and vial were broken and all components were mixed at room temperature, THF was removed under vacuum and then reaction vessel was sealed off. Ampoule containing reacting mixture was placed into a thermostat (120 °C) for about 24 h. The resulting polymer was dissolved in CH<sub>2</sub>Cl<sub>2</sub> and precipitated into methanol, separated by filtration and washed several times with methanol. Mass of the vacuum dried product was equal to 11.9 g (80 % yield).

### Preparation of stereocomplexes

0.5 g of the linear or star-shaped (*R*)-PLA and (*S*)-PLA respectively was dissolved separately in 50 mL of methylene chloride. Then the solutions were mixed together and stirred vigorously during at least 2 hours at room temperature. Then the (*R*)-PLA/(*S*)-PLA/CH<sub>2</sub>Cl<sub>2</sub> resulting mixture was slowly precipitated into the excess of methanol. The fine precipitate of sc-PLA was filtrated and washed a few times with cold methanol and eventually was dried under the dynamic vacuum during 24 h.

### Measurements

#### Size exclusion chromatography (SEC)

Chromatographic system was composed of a 1100 Agilent isocratic pump, a photometer MALLS DAWN EOS (Wyatt Technology Corporation, Santa Barbara, CA), and differential refractometer K-2300 (Knauer). ASTRA 4.90.07 software (Wyatt Technology Corporation) was used for data collecting and processing. Two TSK Gel columns (G 2000 H<sub>XL</sub> and G 6400 H<sub>XL</sub>) were used for separation. Samples were injected as a solution in methylene chloride. The volume of the injection loop was 100 μL. Methylene chloride was used as a mobile phase at flow rate of 0.8 mL · min<sup>-1</sup>. The calibration of the DAWN EOS was carried out by p. a. grade toluene and normalization with a polystyrene standard of 30 000 molar mass. The measurements were carried out at room temperature. SEC analysis was limited to the star-shaped components of stereocomplexes only, because of insolubility of stereocomplexes in the common solvents.

#### NMR

<sup>1</sup>H NMR spectra were recorded in chloroform-d on a Bruker AV200 operating at 200 MHz. Traces of the non-deuterated chloroform were used as an internal standards.

#### Differential Scanning Calorimetry (DSC)

DSC analysis were performed under N<sub>2</sub> at a heating and cooling rate equal to 10 °C · min<sup>-1</sup> on DSC 2920 Modulated TA Instrument. Both temperature and heat flow were calibrated with indium.

## RESULTS AND DISCUSSION

### Molar masses of PLAs

Thus, the star-shaped (*S*)-PLA and (*R*)-PLA enantiomers with 6, ~13, 24 and 32 arms have been obtained. The set of PLA stars was complemented with the linear PLAs of opposite configurations and different molar masses (see Table 1).

The absolute molar masses of star-shaped and linear PLAs were measured by means of the SEC system and, for the PLA arms shorter enough, were determined from

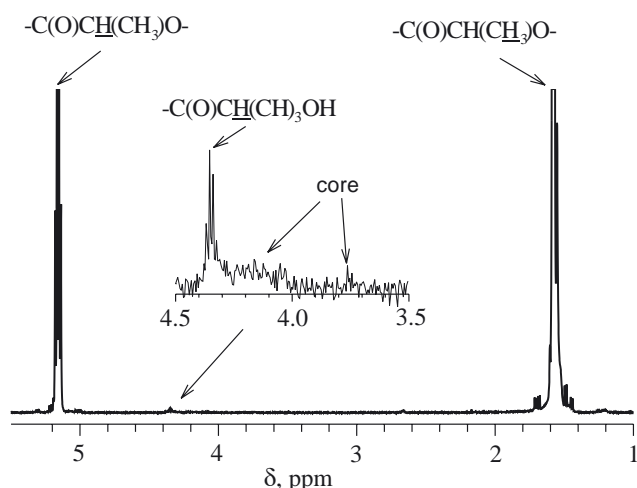


Fig. 1.  $^1\text{H}$  NMR spectrum of 24 arm star-shaped (S)-PLA used to the molar mass calculation. Assignment of signals was done directly in the figure

the  $^1\text{H}$  NMR spectra. An example of  $^1\text{H}$  NMR spectrum used for molar mass calculation for 24-arm star-shaped (S)-PLA is shown in Fig. 1. It was assumed that all -OH groups participated in polymerization. The relative intensity of all lactide units  $[-\text{C}(\text{O})\text{CH}(\text{CH}_3)-]$  from backbone chain equal to  $N_{LA}$  plus relative integration of the end groups  $[-\text{C}(\text{O})\text{CH}(\text{CH}_3)\text{-OH}]$  equal to 1 times the number of functional groups in the initiator (number of arms —  $n$ ) times the molar mass of lactoyl unit (72.065) plus the core molar mass ( $M_{core}$ ) give the total molar mass of star-shaped PLA:

$$M_n(\text{NMR}) = (N_{LA} + 1) \cdot n \cdot 72.056 + M_{core} \quad (1)$$

Table 1. Molar masses of linear and star-shaped PLAs with various number of arms used as components of stereocomplexes

Entry	Number of arms	$M_n \cdot 10^{-3}$ g/mol (Calcd <sup>a</sup> )	$M_n \cdot 10^{-3}$ g/mol (NMR)	$M_n \cdot 10^{-3}$ g/mol SEC	$M_w/M_n$ SEC
I-PLA300(S)	linear	290	—	304	2.24
I-PLA79(S)	linear	79	—	81	1.31
I-PLA79(R)	linear	79	—	85	1.34
I-PLA23(S)	linear	23	—	25	1.20
I-PLA11(S)	linear	11	—	9.7	1.15
I-PLA10(R)	linear	10.5	—	10.3	1.13
s-PLA6(S)	6	100	— <sup>b</sup>	88	1.12
s-PLA6(R)	6	100	— <sup>b</sup>	86	1.11
s-PLA13(S)	13	130	98	125	1.21
s-PLA13(R)	13	130	105	125	1.21
s-PLA24(S)	24	240	260	259	1.52
s-PLA24(R)	24	240	240	224	1.51
s-PLA32(S) <sup>c</sup>	32	300	291	377	1.20
s-PLA32(R)	32	300	285	356	1.21

<sup>a</sup>) — Calculated from  $[M]_0/[I]_0$ .

<sup>b</sup>) — Too high arm molar mass to calculate from  $^1\text{H}$  NMR.

<sup>c</sup>) — Number of arms determined also in ref. [18].

Quality of the  $^1\text{H}$  NMR spectra of the 6-arm PLA was not good enough to use it for molar mass determination because of high molar mass of the single arm of this star ( $\sim 15\,000$ ). Therefore, the signal expected to come from the end groups  $[-\text{C}(\text{O})\text{CH}(\text{CH}_3)\text{-OH}]$  disappeared in the spectrum baseline. The structure of 32-arm star-shaped PLA was supported additionally by the kinetic measurements as described elsewhere [22]. Thus, it was confirmed that for initiators with the number of functional groups  $\leq 32$  practically all of them initiate PLA polymerization. Because of insolubility of the stereocomplexes in common solvents the molar mass measurements were carried out for their starting, homochiral components only. Molar masses determined for linear and star-shaped PLA are collected in Table 1.

### Thermal properties of stereocomplexes

Stereocomplexes were prepared by precipitation of the mixture of enantiomerically pure solutions of (R)- and (S)-PLA into methanol as described in the experimental part or by the simple blending and annealing of the homochiral components in the melt as was described previously [14]. Thermal properties of thus obtained stereocomplexes were analyzed in DSC. The selected examples of DSC thermograms of stereocomplexes with complemented thermograms of their starting components obtained by precipitation from solutions of 6-arms,  $\sim 13$ -arms and mixed linear — star-shaped stereocomplexes are shown in Figs. 2, 3, 4 and 5, respectively. In all presented instances only one endothermic melting peak ( $T_{msc}$ ) for stereocomplexes were observed at the temperature much higher than the melting temperature of their components. The same thermal behavior was observed for stereocomplexes consisting of 24 and 32 arm star-shaped PLAs (not shown here).

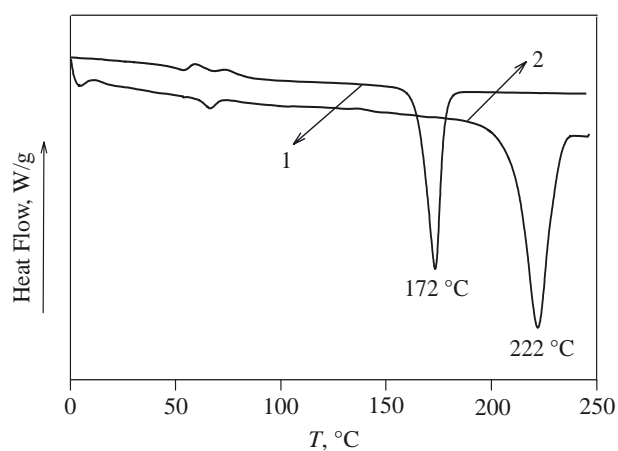


Fig. 2. DSC thermograms of: 1 — 6-arm (S)-PLA [s-PLA6(S)] (see table 1), 2 — stereocomplex of 6-arm star-shaped (S)-PLA and (R)-PLA (sc-PLA6); molar ratio of repeating units 1:1 (first run in DSC, stereocomplex from solution, heating rate  $10\,^\circ\text{C} \cdot \text{min}^{-1}$ )

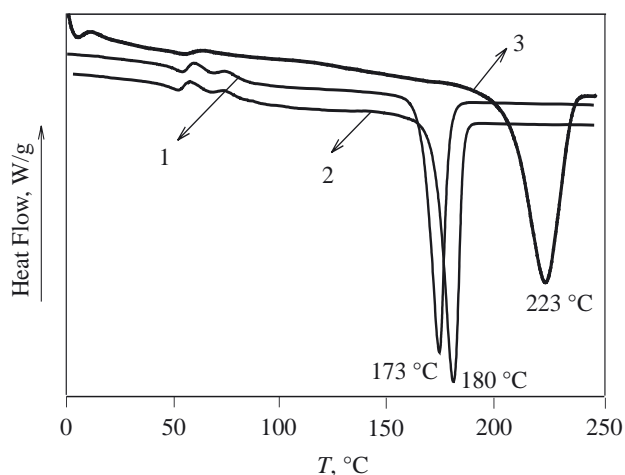


Fig. 3. DSC thermograms of: 1 — 6-arm (S)-PLA [*s*-PLA6(S)] (see table 1), 2 — linear (R)-PLA ( $M_n \sim 10^5$  g/mol) [*l*-PLA100(S)], 3 — stereocomplex of 6-arm star-shaped (S)-PLA and linear (R)-PLA ( $M_n \sim 10^5$  g/mol) (sc-PLA-1); molar ratio of repeating units 1:1 (first run in DSC, stereocomplex from solution, heating rate  $10^\circ\text{C} \cdot \text{min}^{-1}$ )

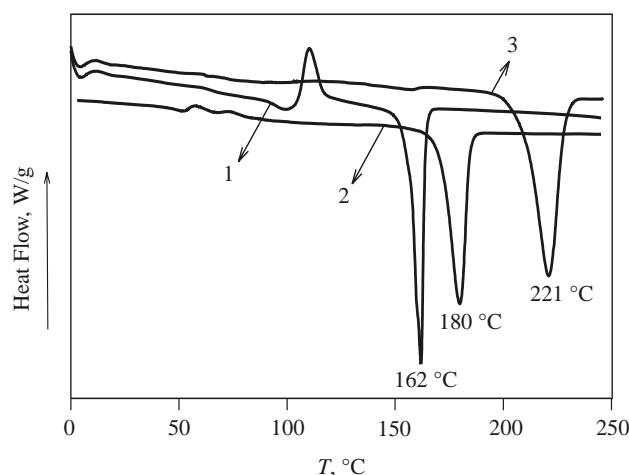


Fig. 5. DSC thermograms of: 1 — 13-arm star-like (S)-PLA [*s*-PLA13(S)], 2 — linear (R)-PLA ( $M_n \sim 10^5$  g/mol) [*l*-PLA100(S)], 3 — stereocomplex of 13-arm star-like (S)-PLA and linear (R)-PLA ( $M_n \sim 10^5$  g/mol) (sc-PLA13-la); molar ratio of repeating units 1:1 (first run in DSC, stereocomplex from solution, heating rate  $10^\circ\text{C} \cdot \text{min}^{-1}$ )

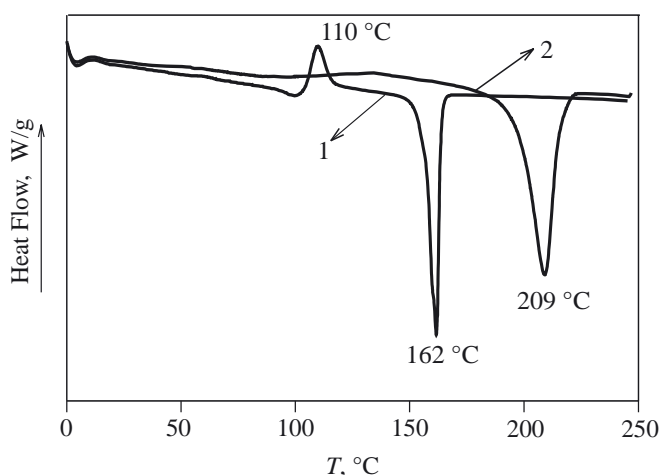


Fig. 4. DSC thermograms of: 1 — 13-arm star-shaped (S)-PLA [*s*-PLA13(S)], 2 — stereocomplex of 13-arm star-shaped (S)-PLA and (R)-PLA (sc-PLA13); molar ratio of repeating units 1:1 (first run in DSC, stereocomplex from solution, heating rate  $10^\circ\text{C} \cdot \text{min}^{-1}$ )

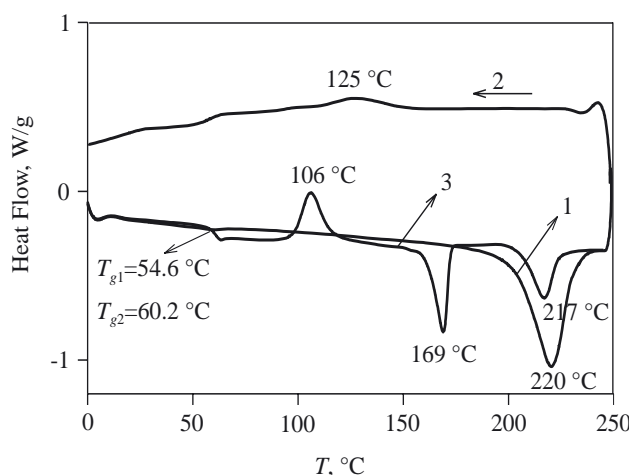


Fig. 6. DSC thermograms of stereocomplex consist of 6-arm (S)-PLA and (R)-PLA (sc-PLA6) obtained from solution (molar ratio of repeating units 1:1): 1 — first run of heating (annealed for 2 min at  $250^\circ\text{C}$  after first run), 2 — cooling to  $0^\circ\text{C}$ , 3 — second run of heating (heating and cooling rate  $10^\circ\text{C} \cdot \text{min}^{-1}$ )

First, thermal stability of star-shaped stereocomplexes obtained by precipitation from solution was analyzed in DSC according to the procedure: heating — cooling — heating. After the first run (heating) the sample was annealed for 2 min at  $\sim 250^\circ\text{C}$  (*i.e.*  $\sim 30^\circ$  above its  $T_{msc}$ ), cooled to  $0^\circ\text{C}$  and then heated once again. In Fig. 6 the corresponding three DSC thermograms for stereocomplex of 6-arm star-shaped PLAs are shown. The melting enthalpy measured for stereocomplex during the first run was very high ( $\Delta H_{msc} = 89.7 \text{ J} \cdot \text{g}^{-1}$ ) comparing with the known enthalpy of fusion for perfectly crystalline linear PLA ( $\Delta H_{mhc}^0 = 93.6 \text{ J} \cdot \text{g}^{-1}$ ) [23]. However, Tsuji and Ikada reported that  $\Delta H_{msc}^0$  value for the stereocomplex crystals having an infinite thickness [ $\Delta H_{msc}^0$

(100 %)] for linear PLA is much higher and equals to  $146 \text{ J} \cdot \text{g}^{-1}$  [24]. This result suggests that crystallinity of the stereocomplex sample of 6-arm star-shaped PLA is equal to 61.4 %.

The second heating in DSC clearly indicated that the stereocomplex of 6-arm star-shaped PLA is restored only partially because the additional endothermic peak appeared for melting of homo crystallites at  $169^\circ\text{C}$  ( $\Delta H_{mhc} = 26.7 \text{ J} \cdot \text{g}^{-1}$ ) and the stereocomplex endothermic peak at  $217^\circ\text{C}$  exhibited much lower value of melting enthalpy ( $\Delta H_{msc} = 22.8 \text{ J} \cdot \text{g}^{-1}$ ). Then the total sample crystallinity (homo and stereocomplex crystallites) measured during the second run is 44.1 % only.

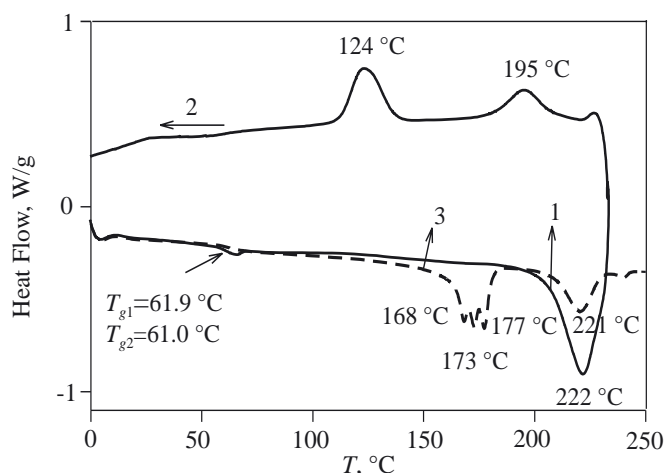


Fig. 7. DSC thermograms of stereocomplex consists of 6-arm (S)-PLA and linear (R)-PLA (sc-PLA6-l) obtained from solution (molar ratio of repeating units 1:1): 1 — first run at heating (annealed for 2 min at 235 °C), 2 — cooling to 0 °C, 3 — second run at heating (heating and cooling rate 10 °C · min<sup>-1</sup>)

The same behavior was observed for mixed stereocomplexes: 6-arm star (S)-PLA — linear (R)-PLA (Fig. 7) and 13 arms star (S)-PLA — linear (R)-PLA (not shown here) where molar mass of linear components is equal to  $\sim 10^5$  g/mol with 1:1 molar ratio PLA repeating units in star-shaped and linear polymers. The stereocomplexes composed of star-shaped components (or mixed: star-linear) described above are easy to obtain by precipitation from the solution but after the first run (heating) in DSC and annealing for 2 min at  $\sim 250$  °C during the second heating two pairs of endothermic peaks appeared. In the case of the mixed stereocomplex:  $\sim 13$ -arms PLA — linear PLA the first two peaks at lower temperature (170 °C and 177 °C) are related to melting of star-shaped and linear enantiomeric components and other peaks at higher temperature (222 °C and 237 °C) were correlated with melting of stereocomplex crystallites with different structural arrangement (thermograms not shown here).

These observations are in contrast to the thermal behavior of stereocomplexes of star-shaped poly(lactide)s with higher (than six) number of arms (*i.e.*  $\sim 13$ , 24 and 32). In Fig. 8 the DSC thermograms of 24-arm star-shaped sc-PLAs are shown. In the first thermal run (heating) only one endothermic peak appeared at 214 °C with high  $\Delta H_{msc} = 79.1$  J · g<sup>-1</sup>. After annealing for 2 min at 235 °C the cooling run was recorded and the crystallization peak at 104 °C was observed. In the second run (heating) also single melting peak is present only, although both melting temperature and melting enthalpy are lower than for the starting sample. The similar thermograms were also recorded for  $\sim 13$ - and 32-arm star-shaped stereocomplexes. It should also be stressed that an average molar mass of arms in all analyzed star-shaped poly(lactide)s is almost the same and equal to  $\sim 10$  000 g/mol.

The same temperature regime was used for recording thermograms of linear sc-PLAs with different molar masses prepared separately for comparison. The following thermal data in DSC first run were found for stereocomplexes from solution:  $T_{msc} = 223$  °C;  $\Delta H_{msc} = 86.6$  J · g<sup>-1</sup> for  $M_n \cong 10^4$  g/mol and  $T_{msc} = 227$  °C,  $\Delta H_{msc} = 55.7$  J · g<sup>-1</sup> for  $M_n \cong 10^5$  g/mol.

The inspection of the literature [23—29] and Tables 2 and 3 indicates that the melting temperature of the linear PLAs depends on the molar mass and for high molar mass ( $M_n \geq 10^5$  g/mol)  $T_m$  is around 180 °C. However, the melting temperature of star-shaped PLA is generally lower and slight influence of the arm number on the melting temperature is observed. For 6-arm star-shaped PLA ( $M_n \cong 8.0 \cdot 10^5$  g/mol)  $T_m = 172$  °C (see Fig. 2)

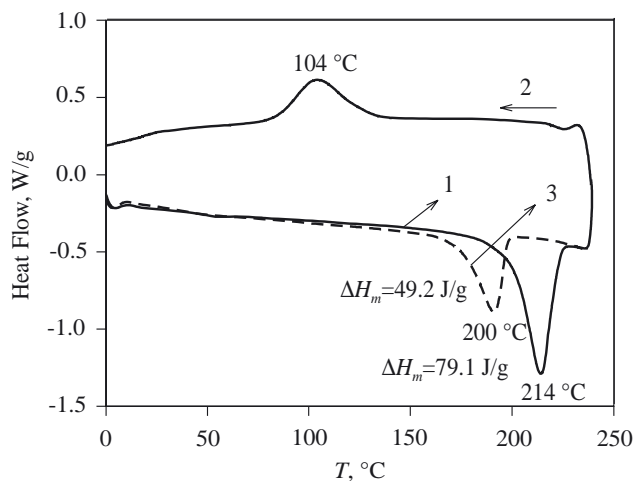


Fig. 8. DSC thermograms of stereocomplex of star-shaped PLA with 24 arms (sc-PLA24) obtained from solution. Three runs in DSC: heating (1) — cooling (2) — heating (3); annealed for 2 min at 250 °C after first run (heating and cooling rate 10 °C · min<sup>-1</sup>)

although for PLA with  $\sim 13$  and higher (*i.e.* 24-, 32-) number of arms ( $M_n \geq 10^5$  g/mol)  $T_m = \sim 162$  °C (see Fig. 4 and Table 2). Melting temperature is always higher for stereocomplex samples of PLAs prepared by precipitation from solution than for the melted samples during the first run in DSC, when measured in the second run (see Fig. 8). This means, that crystallites of stereocomplex prepared from solution are more perfect.

It is known that in order to prepare stereocomplex crystallites from perfectly uniform linear (R)-PLA and (S)-PLA at least seven pairs of interacting sequential units in (S)-PLA and (R)-PLA chains are needed but in the case of homo-crystallites eleven lactide sequential units from the different chains have to interact each with other [30]. However, Muellen *et al.* found for star-shaped (S)-PLAs that the star-shaped architecture frustrate the crystallization process and requires a larger number of repeating units (at least 50) for crystallization to occur

**Table 2.** Thermal parameters (from DSC) of star-shaped PLA stereocomplexes and their (R)-PLA and (S)-PLA components (second run after fast cooling to room temperature from the melt, annealed for 2 min at 250 °C, heating rate 10 °C · min<sup>-1</sup>)

Entry	Number of arms	$M_n \cdot 10^{-3}$ g/mol	$T_g$ , °C	$T_{cc}^*)$ , °C	$T_m$ , °C	$\Delta H_{cc}^*)$ , J · g <sup>-1</sup>	$\Delta H_m$ , J · g <sup>-1</sup>
s-PLA6(S)	6	88	58.6	115	170	-40.2	39.7
s-PLA6(R)	6	86	62.4	121	175	-35.2	35.8
sc-PLA6 <sup>**</sup> )	6	~87	61.0	110	171.2/219.5	-40.3/-4.5	29.7/18.4
sc-PLA6-l <sup>**</sup> )	6+linear	88/85	61.7	110	172/178/220	-42.0	30.3/12.9
s-PLA13(S)	~13	125	60.6	130	165	-36.5	36.9
s-PLA13(R)	~13	125	60.1	127	161	-40.8	38.4
sc-PLA13	~13	125	47.7	75	204	-56.0	55.0
sc-PLA13-l	~13+linear	125/10	49.3	77	213	-59.0	58.0
sc-PLA13-la <sup>***</sup> )	~13+linear	125/100	57.3	89/103/188	163/174/217	-34.5/-5.4	4.1/4.8/30.4
s-PLA24(S)	24	259	60.3	125	163	-38.5	39.0
s-PLA24(R)	24	224	60.4	125	165	-38.9	39.6
sc-PLA24	24	~240	42.6	74	199	-51.0	51.2
s-PLA32(S)	32	377	59.7	109	165	-46.6	46.9
s-PLA32(R)	32	356	59.3	106	164	-47.3	47.4
sc-PLA32	32	~360	50.1	85	200	-47.1	47.9

<sup>\*)</sup> —  $T_{cc}$  — cold crystallization temperature,  $\Delta H_{cc}$  — enthalpy of cold crystallization.

<sup>\*\*</sup>) — Two melting peaks are observed for stereocomplex and their components [star (S)-PLA and (R)-PLA melting peaks overlapped].

<sup>\*\*\*</sup>) — Three melting peaks are observed for stereocomplex and their components [star (S)-PLA and linear (R)-PLA melting peaks appeared separately].

[31]. The lower number of the interacting lactide units needed and the higher energy of interaction (hydrogen bonds against van der Waals interactions) may facilitate crystallization of stereocomplexes.

**Table 3.** Thermal parameters (from DSC) of linear PLAs with various molar mass and their linear stereocomplexes (the second run after fast cooling to room temperature from the melt annealed for 2 min at 250 °C, heating rate 10 °C · min<sup>-1</sup>)

Entry	$M_n \cdot 10^{-3}$ g/mol	$T_g$ , °C	$T_{cc}^*)$ , °C	$T_m$ , °C	$\Delta H_{cc}^*)$ , J · g <sup>-1</sup>	$\Delta H_m$ , J · g <sup>-1</sup>
l-PLA300(S)	304	60.9	105	178	-34.5	36.7
l-PLA100(S)	81	59.3	124	172	-45.8	46.2
l-PLA100(R)	85	61.0	113	180	-47.9	46.9
l-PLA25(S)	25	47.3	88	169	-51.4	52.1
l-PLA10(S)	9.7	55.8	90	162	-54.6	54.4
l-PLA10(R)	10.3	57.4	93	168	-53.2	53.4
sc-lPLA100	~80	61.4	108	176/219	-52.0	30.4/22.0
sc-lPLA10	~10	60.0	84	225	-72.4	71.5

<sup>\*)</sup> Meanings of  $T_{cc}$  and  $\Delta H_{cc}$  — see table 2.

To explain the observed enhanced stability of stereocomplexes in the melt another thermal experiment was performed. After the first heating in DSC, samples were annealed for 2 min at 250 °C to erase their thermal history and then rapidly cooled down to the room temperature. It is known that PLA samples after melting to the isotropic form and then cooling rapidly (> 20 °C · min<sup>-1</sup>) are completely amorphous [32]. It has therefore been intended to “freeze” the melting state of the samples. Then the next heating run in DSC was recorded. Eventually the same thermal treatment was applied to enantiomeric components of stereocomplexes. In Fig. 9 the thermo-

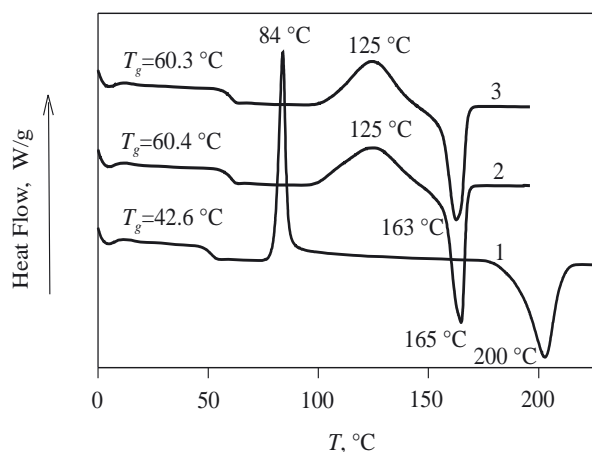


Fig. 9. DSC thermogram of stereocomplex (1) consists with 24-arm (S)-PLA and (R)-PLA (molar ratio of repeating 1:1) and thermograms of 24-arm (S)-PLA [s-PLA24(S)] (2) and 24-arm (R)-PLA [s-PLA24(R)] (3) enantiomeric components. The second runs in DSC are shown after melting and annealing for 2 min in the first run at 250 °C and rapid cooling to the room temperature to preserved an amorphous structure (heating rate 10 °C/min, cooling rate — much higher than 20 °C · min<sup>-1</sup>)

grams for 24-arm star-shaped sc-PLA and its enantiomeric components are shown. The  $T_g$  of enantiomeric star-shaped components of sc-PLA is almost the same and equal to 60.3 °C and 60.4 °C respectively. The broad cold crystallization peak appeared at 125 °C for both 24-arm star-shaped (R)-PLA and 24-arm star-shaped (S)-PLA and then the melting endothermic peak was observed at 163 °C and 165 °C respectively. The  $T_g$  for sc-PLA of 24-arm stars is equal to 42.6 °C then very sharp

cold crystallization peak appeared at low temperature (at 84 °C). Eventually, the sc-PLA crystallites melt at 200 °C.

The lower  $T_g$  for sc-PLAs than that for their enantiomeric star-shaped components starting from the star with ~13 arms and more (see Fig. 9 and Table 2) suggests higher free volume in an amorphous phase of stereocomplexes than in an amorphous phase of pure enantiomers. This result contradicts some reported results [33] and the intuitive picture of the "heterogenic" stereocomplex amorphous phase which should show the higher ordering [because of (R)-PLA and (S)-PLA interactions] than its "homogenic" counterpart; thus one should expect the higher  $T_g$ . One of the possible explanations is as follow. The strong intermolecular interactions of the enantiomeric chains of star-shaped PLAs created pairs of chains that keep a few macromolecules together lead to stereocomplex aggregates (i.e. stereocomplex

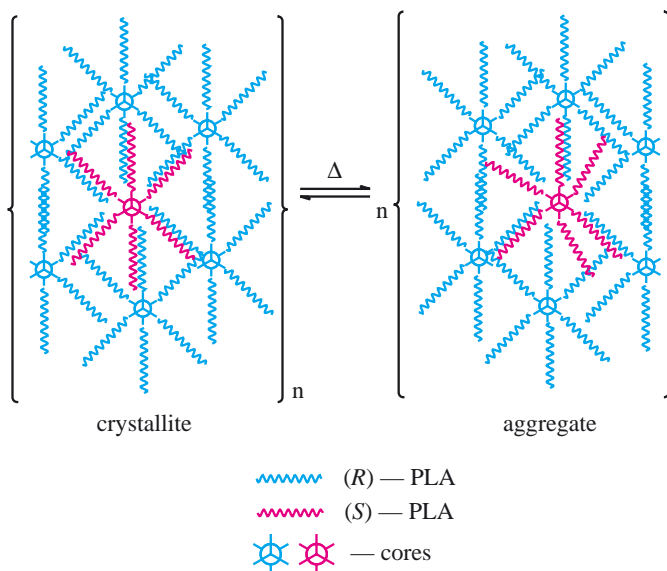


Fig. 10. Scheme of the creation of aggregates in the molten state. The strong intermolecular interactions of the enantiomeric chains of star-shaped PLAs keep a few macromolecules together even in the molten state at high temperature (see text)

"precursors") even in the molten state at high temperature. Therefore the internal part of the resulting aggregate has higher density than the external one (see Fig. 10). Polylactide chains engaged in stereocomplex bonds formation (internal chains) do not participate in the glass transition. Thus the free volume of the fraction of external chains (which do not interact in the stereocomplex aggregates) creating an amorphous phase is higher than it is in the fully isotropic homogenic amorphous phase. Therefore, the higher free volume favors the faster relaxation at the lower  $T_g$ . The similar influence of the chain configuration on  $T_g$  was observed for isotactic and

atactic poly(methyl methacrylate) ( $T_g$  of isotactic isomer is lower than atactic one) [34].

On the other hand, the  $T_{ccsc}$  (cold crystallization peak of stereocomplex) is very sharp and appears at much lower temperature than the broad cold crystallization peaks for (S)-PLA and (R)-PLA components. For samples of the star-shaped PLA melted in the first DSC run, then fast cooled to room temperature, and finally melted in the second DSC run, the enthalpy of the cold crystallization ( $\Delta H_{cc}$ ) and then the enthalpy of the melting ( $\Delta H_m$ ) are almost identical (see Table 2). This observation strongly suggests that all samples analyzed according to above described procedure were purely amorphous before the second heating run.

In a solid amorphous sample of polymer below  $T_g$ , the chain motions are restricted to vibrations around fixed positions. From the formal point of view there is a liquid state of polymer above  $T_g$  and below  $T_{cc}$  if below  $T_g$  the sample was fully amorphous. In these conditions (extremely viscous liquid) the translational motions of polymer segments are limited and require much longer time to crystallize. This is additional proof suggesting that in the case of stereocomplexes of star-shaped PLA some seeds of crystallites of the stereocomplex (i.e. aggregates) survived in the melt and being able to fast crystallize even in exceptionally viscous state. The higher number of nucleating centers results in the faster rate of the crystallization and the lower  $T_{cc}$ . On the other hand, the cold crystallization of homochiral components requires higher temperatures and longer time under the same rate of heating ( $10\text{ °C} \cdot \text{min}^{-1}$ ) (see Fig. 9). The melting peaks of stereocomplexes are broader than the melting peaks of (S)- and (R)-PLA components. It means that the distribution of dimensions of stereocomplex crystal-

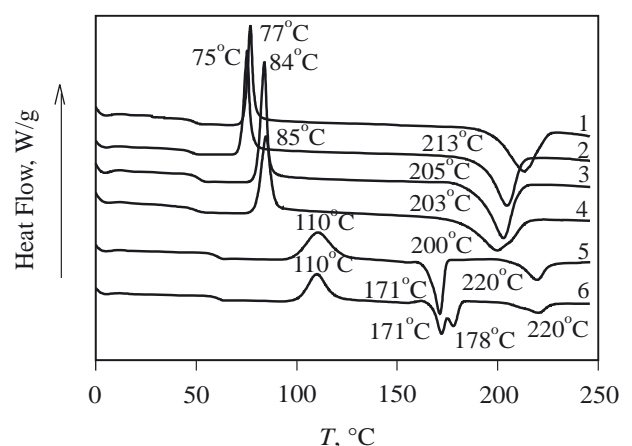


Fig. 11. DSC thermograms of stereocomplexes of star-shaped PLAs with various number of arms: 1 — 13-arms + linear, 2 — 13-arms, 3 — 24-arms, 4 — 32-arms, 5 — 6-arms, 6 — 6-arms + linear. The second runs in DSC are shown after melting and annealing for 2 min in the first run at 250 °C and rapid cooling to room temperature to preserved an amorphous structure (heating rate  $10\text{ °C} \cdot \text{min}^{-1}$ , cooling rate — much higher than  $20\text{ °C} \cdot \text{min}^{-1}$ )

lites are broader than that for homochiral crystallites because faster crystallization results in higher dimension dispersity.

The same enhancement of thermal stability was observed for stereocomplexes composed of star-shaped PLAs with ~13 and 32 arms and for mixed linear — star-shaped stereocomplex with ~13 arms when  $M_n$  of the linear component is equal to  $10^4$  g/mol and contrary to the 6-arm star, as it is seen in Fig. 11. It seems that the number of arms in the star-shaped components of sc-PLA plays an important role in an enhancement of interactions between arms of stars with the opposite configuration. The appropriately high number of arms is required to provide the effective cooperative interactions of chains and in the consequence leads to the high thermal stability of star-shaped stereocomplexes.

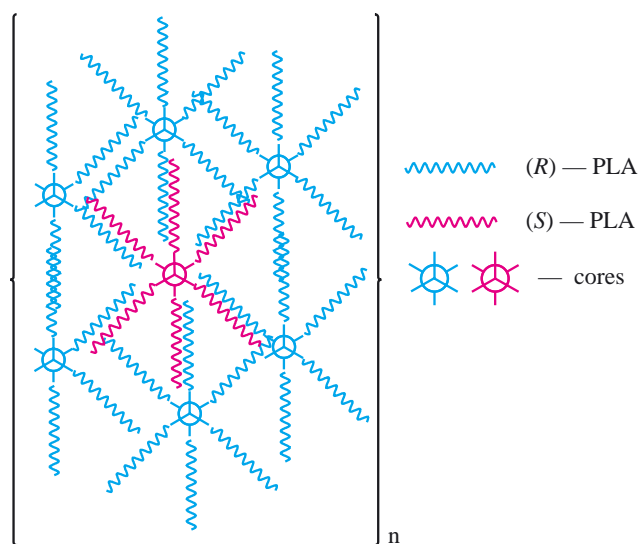


Fig. 12. Schematic structure the antiparallel stereocomplexes of the star-shaped macromolecules

Two polylactide chains, because of their asymmetry, can interact in two manners: parallelly and antiparallelly. In the case of the linear sc-PLAs both mentioned above types of interactions are possible, although according to Cantov *et al.* calculations [35], interaction energy is higher for the parallelly oriented PLA helices. However, these calculations giving the advantage of parallel interaction of (R)-PLA and (S)-PLA in the linear stereocomplexes may not fully apply to the star-shaped structures. In the star-shaped sc-PLA chains may predominantly interact in the antiparallel manner because of the fixation of the chain geometry as shows in Fig. 12. The steric hindrance in stars rather excluded the parallel arm interactions.

#### CONCLUSIONS

It has been shown that equimolar mixtures of PLA macromolecules with opposite chirality having star-

shaped architectures have the advantage of fast crystallization into the stereocomplex crystallites when compared to their linear counterparts. It was also indicated that the mixed stereocomplexes of star-shaped and linear PLAs can be obtained under similar conditions.

It has been observed that both the low molar mass linear polymers as well as multi-arm stars with relatively short arms, when cooled continuously from the melt or heated after rapid cooling from the melt, can more easily form the stereocomplex crystallites than longer linear PLAs and star-shaped PLAs with lower number of arms (*i.e.* six arms). In the later two instances always considerable fraction of the homochiral crystallites has been formed. These effects are explained by differences in the mobility of polymer chains in these systems as a result of cooperative interactions of many helical arms in the PLA stars.

The cooperative formation of many stereocomplex pairs of chains in the frame of interacted enantiomeric star-shaped PLAs with adequate number of arms enhances the thermal stability of their stereocomplex crystallites. Part of the stereocomplex aggregates can probably survive in the melt and then crystallize very fast during second heating in DSC even at the relatively low temperature near  $T_g$ .

#### ACKNOWLEDGEMENTS

The financial support the Polish Ministry of Scientific Research and Information Technology grant 3T09A 002 27 (2004—2007) is gratefully acknowledged. The author of this paper thanks Prof. Stanislaw Penczek for useful comments and discussions. Special thanks are to professor A. Fradet for providing a sample of polyester dendrimer G-3 (with 24 -OH groups).

#### REFERENCES

1. Gruber P., O'Brien M.: "Polylactides NatureWorks™ PLA." in "Biopolymers. Polyesters III — Applications and Commercial Products" (Ed. Steinbuechel A., Doi Y.), Wiley-VCH, Weinheim, 2001, Vol. 4, 235—249.
2. Kawashima N., Ogawa S., Obuchi S., Matsuo M., Yagi T.: "Polylactic acid «LACEA»" in [1], 251—274.
3. Duda A., Penczek S.: *Polimery* 2003, **48**, 16.
4. Słomkowski S., Gadzinowski M., Sosnowski S., Radomska-Galant I.: *Polimery* 2005, **50**, 546.
5. Gałęski A., Piórkowska E., Pluta M., Kuliński Z., Masirek R.: *Polimery* 2005, **50**, 562.
6. Ikada Y., Jamshidi K., Tsuji H., Hyon S.-H.: *Macromolecules* 1987, **20**, 904.
7. Zhang J., Sato H., Tsuji H., Noda I., Ozaki Y.: *Macromolecules* 2005, **38**, 1822.
8. Sarausa J.-R., Rodriguez N. L., Arraiza A. L., Meaurio E.: *Macromolecules* 2005, **38**, 8353.
9. Tsuji H., Hori F., Hyon S.-H., Ikada Y.: *Macromolecules* 1991, **24**, 2719.

10. Tsuji H., Hyon S.-H., Ikada Y.: *Macromolecules* 1991, **24**, 5651.
11. Tsuji H., Hyon S.-H., Ikada Y.: *Macromolecules* 1991, **24**, 5657.
12. Tsuji H., Ikada Y.: *Macromolecules* 1991, **24**, 5657.
13. Fukushima K., Kimura Y.: *Polym. Intern.* 2006, **55**, 626.
14. Biela T., Duda A., Penczek S.: *Macromolecules* 2006, **39**, 3710.
15. Bednarek M., Kubisa P., Penczek S.: *Macromolecules* 2001, **34**, 5112.
16. Chikh L., Arnaud X., Guillermain C., Tessier M., Fradet A.: *Macromol. Symp.* 2003, **199**, 209.
17. Biela T., Duda A., Penczek S., Rode K., Pasch H.: *J. Polym. Sci., Part A: Polym. Chem.* 2002, **40**, 2884.
18. Biela T., Duda A., Rode K., Pasch H.: *Polymer* 2003, **44**, 1851.
19. Kowalski A., Duda A., Penczek S.: *Macromolecules* 2000, **33**, 7359.
20. Duda A.: *Polimery* 2002, **47**, 469.
21. Biela T., Duda A., Penczek S.: *Macromol. Symp.* 2002 **181**, 1.
22. Kowalski A., Libiszowski J., Biela T., Cypriak M., Duda A., Penczek S.: *Macromolecules* 2005, **38**, 8170.
23. Fischer E. W., Sterzel H. J., Wegner G. K. -ZuZ: *Polymere* 1973, **251**, 980.
24. Tsuji H., Hori F., Nakagawa M., Ikada Y., Odani H., Kitamaru R.: *Macromolecules* 1992, **25**, 4114.
25. Jamshidi K., Hyon S.-H., Ikada Y.: *Polymer* 1988, **29**, 2229.
26. Spinu M., Jackson C., Keating M. Y., Gardner K. H.: *J. Macromol. Sci. — Pure Appl. Chem.* 1996, **A33(10)**, 1497.
27. Kim S.-H., Kim Y.-H.: *Macromol. Symp.* 1999, **144**, 277.
28. Korhonen H., Helminen A., Sappala J.-V., *Polymer* 2001, **42**, 7541.
29. Lee S.-H., Kim S.-H., Han Y.-K., Kim Y.-H.: *J. Polym. Sci.: Part A: Polym. Chem.* 2001, **39**, 973.
30. De Jong S. J., Van Dijk-Wolthuis W. N. E., Kettenes-van den Bosch J. J., Schuyl P. J. W., Hennink W. E.: *Macromolecules* 1998, **31**, 6397.
31. Klok H.-A., Becker S., Schuch F., Pakula T., Muellen K.: *Macromol. Biosci.* 2003, **3**, 727.
32. Miyata T., Masuko T.: *Polymer* 1998, **39**, 5515.
33. Schneider H.-A. J.: *Res. Natl. Inst. Stand. Technol.* 1997, **102**, 229.
34. Riande E., Diaz-Calleja R., Prolongo M. G., Masegosa R. M., Salom C.: "Polymer Viscoelasticity. Stress and Strain in Practice", Marcel Dekker, Inc. New York, Basel, 2000, Chapter 2, pp. 29—83.
35. Brizzolara D., Cantow H.-J., Diederichs K., Keller E., Domb A. J.: *Macromolecules* 1996, **29**, 191.

Received 31 VIII 2006.